Defining the Binding Site of Levosimendan and Its Analogues in a Regulatory Cardiac Troponin C−Troponin I Complex[†]

Ian M. Robertson, Olga K. Baryshnikova, Monica X. Li, and Brian D. Sykes*

Department of Biochemistry, University of Alberta, Edmonton, Alberta, Canada T6G 2H7

Received March 14, 2008; Revised Manuscript Received May 26, 2008

ABSTRACT: The interaction of Cardiac Troponin C (cTnC) and Cardiac Troponin I (cTnI) plays a critical role in transmitting the Ca^{2+} signal to the other myofilament proteins in the activation of cardiac muscle contraction. As such, the cTnC−cTnI interface is a logical target for cardiotonic agents such as levosimendan that can modulate the Ca^{2+} sensitivity of the myofilaments. Evidence indicates that drug candidates may exert their effects by targeting a site formed by binding of the switch region of cTnI to the regulatory N domain of cTnC (cNTnC). In this study, we utilized two-dimensional $^{1}H-^{15}N$ HSQC NMR spectroscopy to monitor the binding of levosimendan and its analogues, CMDP, AMDP, CI-930, imazodan, and MPDP, to cNTnC·Ca^{2+} in complex with two versions of the switch region of cTnI ($cTnI_{147-163}$ and $cTnI_{144-163}$). Levosimendan, CMDP, AMDP, and CI-930 were found to bind to both cNTnC·Ca^{2+}·$cTnI_{147-163}$ and cNTnC·Ca^{2+}·$cTnI_{144-163}$ complexes. These compounds contain a methyl group that is absent in MPDP or imazodan. Thus, the methyl group is one of the pharmacophores responsible for the action of these pyridazinone drugs on cTnC. Furthermore, the results showed that the cNTnC·Ca^{2+}·$cTnI_{144-163}$ complex presents a higher-affinity binding site for these compounds than the cNTnC·Ca^{2+}·$cTnI_{147-163}$ complex. This is consistent with our observation that the affinity of $cTnI_{144-163}$ for cNTnC·Ca^{2+} is ∼10-fold stronger than that of $cTnI_{147-163}$, likely a result of electrostatic forces between the N-terminal RRV extension in $cTnI_{144-163}$ and the acidic residues in the C and D helices of cNTnC. These results will help in the delineation of the mode of action of levosimendan on the important functional unit of cardiac troponin that constitutes the regulatory domain of cTnC and the switch region of cTnI.

Regulation of cardiac muscle contraction by intracellular Ca^{2+} is critical for normal heart function. This important task is accomplished by the heterotrimeric troponin complex anchored on the thin filament by its tropomyosin-binding subunit cTnT.[1] The inhibitory subunit cTnI acts as a molecular switch moving from actin to the Ca^{2+}-binding subunit cTnC as the intracellular Ca^{2+} concentration increases. This switch is essential for transmitting the Ca^{2+} signal to the other myofilament proteins, leading to tension-producing cross bridges between actin and myosin and ultimately activating cardiac muscle contraction (for recent reviews, see refs *1* and *2*).

Structural studies of troponin have helped in the elucidation of the molecular mechanism that governs the switching of cTnI to cTnC. cTnC is an "elongated" molecule with two globular N and C domains connected by a flexible linker in solution (*3*). Apo cNTnC was shown to adopt a "closed" conformation with most of its hydrophobic residues buried (*4*). The energy barrier for "opening" is overcome by the binding of Ca^{2+} and the switch region of cTnI (residues ∼147−163) (*5, 6*). In the NMR structure of the cNTnC·Ca^{2+}·$cTnI_{147-163}$ complex (*6*) and the X-ray structure of the cTnC·$3Ca^{2+}$·$cTnI_{31-210}$·$cTnT_{183-288}$ complex (*7*), $cTnI_{147-163}$ adopts an α-helical conformation and lies across the hydrophobic groove with contacts with key hydrophobic residues in cNTnC. This interaction initiates the movement of the adjoining inhibitory ($cTnI_{128-147}$) and C-terminal ($cTnI_{163-210}$) regions of cTnI away from actin and releases the inhibition of the actomyosin ATPase, leading to muscle contraction (*1*). The $cTnI_{34-71}$ region binds tightly to cCTnC in the absence or presence of cytosolic Ca^{2+}. In the structure of cTnC·$3Ca^{2+}$·$cTnI_{31-210}$·$cTnT_{183-288}$, the region of residues 34−71 of cTnI forms a long α-helix and makes extensive contacts with the hydrophobic surface of cCTnC. Most of the inhibitory region of cTnI is unobserved in cTnC·$3Ca^{2+}$·$cTnI_{31-210}$·$cTnT_{183-288}$, but a similar region of sTnI is shown to have an extended conformation and interact

[†] Supported by the Canadian Institutes of Health Research (Grant MOP 37760), the Heart and Stroke Foundation of Canada, and the National Institutes of Health (Grant R01 HL 085234).

* To whom correspondence should be addressed. Phone: (780) 492-5460. Fax: (780) 492-0886. E-mail: brian.sykes@ualberta.ca.

[1] Abbreviations: TnC, troponin C; cTnC, cardiac troponin C; cNTnC, N domain of cTnC; cCTnC, C domain of cTnC; cTnI, cardiac troponin I; cTnT, cardiac troponin T; sTnC, skeletal troponin C; sNTnC, N domain of sTnC; sTnI, skeletal troponin I; sTnT, skeletal troponin T; K_D, dissociation constant; levosimendan, (−)-[4-(1,4,5,6-tetrahydro-4-methyl-6-oxo-3-pyridazinyl)phenyl]hydrozonopropanedinitrile; CMDP, 6-(4-chlorophenyl)-5-methyl-4,5-dihydro-3(2*H*)-pyridazinone; AMDP (a racemic mixture of the levosimendan metabolite OR-1855), 6-(4-aminophenyl)-5-methyl-4,5-dihydro-3(2*H*)-pyridazinone; CI-930, 4,5-dihydro-6-[4-(1-imidazol-1-yl)phenyl]-5-methyl-4,5-dihydro-3(2*H*)-pyridazinone; imazodan, 4,5-dihydro-6-[4-(1-imidazol-1-yl)phenyl]-3(2*H*)-pyridazinone; MPDP, 6-(4-methoxyphenyl)-4,5-dihydro-3(2*H*)-pyridazinone; W7, *N*-(6-aminohexyl)-5-chloro-1-naphthalenesulfonamide; anapoe, 2-[2-(2-{2-[4-(1,1,3,3-tetramethylbutyl)phenoxy]-ethoxy}ethoxy)ethoxy]ethanol; bepridil, *N*-[3-(2-methylpropoxy)-2-pyrrolidin-1-ylpropyl]-*N*-(phenylmethyl)aniline; Eu-(hfc)$_3$, europium tris[3-(heltafluoropropylhydroxymethylene)-(−)-camphorate]; TMS, tetramethylsilane.

10.1021/bi800438k CCC: $40.75
Published on Web 06/21/2008

with the central helix area of sTnC in the X-ray structure of the sTnC·4Ca^{2+}·$sTnI_{1-182}$·$sTnT_{156-262}$ complex (*8*). Specifically, the inhibitory region of sTnI was found to make electrostatic contacts with the acidic residues on the central DE-helix of sTnC, similar to those observed in the NMR solution structure of cCTnC·2Ca^{2+}·$cTnI_{128-147}$ (*9, 10*).

The Ca^{2+}-sensitive interaction between cNTnC and the switch region of cTnI has been proposed to be an important target for cardiotonic drugs (for reviews, see refs *1* and *11*−*15*). These drugs are useful in the treatment of heart disease associated with depressed cardiac contractility. They act via a mechanism that modulates the Ca^{2+} sensitivity of troponin without an overload of Ca^{2+} that would perturb the regulation of other Ca^{2+}-based signaling pathways in cardiomyocytes, leading to a series of undesirable side effects such as arrhythmia and death. A good example is levosimendan, which has proven to be a well-tolerated and effective treatment for patients with severe decompensated heart failure (for reviews, see refs *13* and *14*). Several cardiotonic agents have been shown to target the binding site formed by cNTnC and the switch region of cTnI. In the NMR structure of the cNTnC·Ca^{2+}·$cTnI_{147-163}$·bepridil complex, bepridil and $cTnI_{147-163}$ bind concurrently to the hydrophobic pocket of the protein (*16*). In the structure of the sTnC·4Ca^{2+}·$sTnI_{1-182}$·$sTnT_{156-262}$ complex, a polyoxyethylene detergent molecule, anapoe, binds to sNTnC together with the switch region of sTnI ($sTnI_{115-131}$). This binding mode is likely responsible for the increase in the contractile force of muscle fibers in the presence of anapoe (*8*). Further, we have shown recently that a calmodulin antagonist, W7, binds to cNTnC and the binding can occur in the presence of the switch region of cTnI (*17*). Thus, these compounds, together with $cTnI_{147-163}$, may exert their effects by altering the dynamic equilibrium between closed and open cNTnC conformations, enhancing the affinity for cTnI and thereby modulating the calcium sensitivity of troponin. Structures of cNTnC·Ca^{2+}·levosimendan or cNTnC·Ca^{2+}·$cTnI_{147-163}$·levosimendan are not yet available. NMR chemical shift mapping has shown that levosimendan's primary binding site is also located in the N domain of cTnC in the presence of cTnI (*13, 18*); however, the exact binding geometry has not been established. To better delineate the binding site of levosimendan in cNTnC, we investigated the binding of levosimendan and its analogues (AMDP, CMDP, CI-930, MPDP, and imazodan) (Figure 1) to cNTnC·Ca^{2+}·$cTnI_{147-163}$ and cNTnC·Ca^{2+}·$cTnI_{144-163}$. $cTnI_{144-163}$ is used because the N-terminal RRV extension relative to $cTnI_{147-163}$ is expected to be important for a network of interactions responsible for the binding of drug molecules, on the basis of structural analysis of the cNTnC·Ca^{2+}·$cTnI_{147-163}$·bepridil and sTnC·4Ca^{2+}·$sTnI_{1-182}$·$sTnT_{156-262}$ complexes. We used two-dimensional (2D) $^{1}H-^{15}N$ HSQC NMR spectral changes to monitor the formation of the cNTnC·Ca^{2+}·$cTnI_{147-163}$ and cNTnC·Ca^{2+}·$cTnI_{144-163}$ complexes and the titration of these complexes with drug molecules. Our results revealed that only those compounds containing the chiral methyl group induced chemical shift changes, suggesting that this group constitutes a key pharmacophore responsible for the binding of pyridazinone derivatives to cNTnC. The findings also showed that the pyridazinone compounds bound to cNTnC·Ca^{2+}·$cTnI_{144-163}$ with a higher affinity than to cNTnC·Ca^{2+}·$cTnI_{147-163}$. This correlates with our observation that the affinity of $cTnI_{144-163}$ for cNTnC·Ca^{2+} is ~10-fold stronger than that of $cTnI_{147-163}$, likely a result of electrostatic forces between the N-terminal RRV extension in $cTnI_{144-163}$ and the acidic residues in the C and D helices of cNTnC.

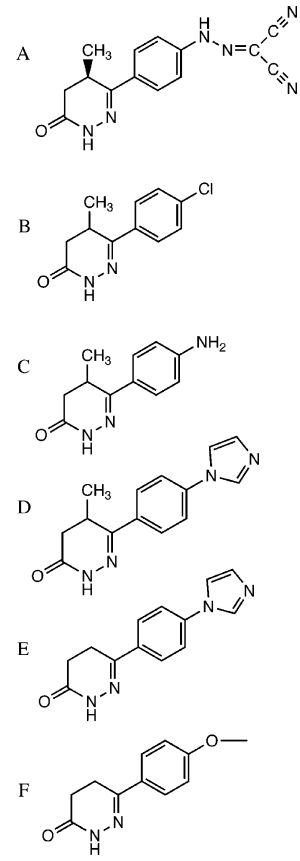

FIGURE 1: Chemical structures of (A) levosimendan, (B) CMDP, (C) AMDP, (D) CI-930, (E) imazodan, and (F) MPDP.

EXPERIMENTAL PROCEDURES

Sample Preparation. Recombinant human cNTnC (residues 1−89) with C35S and C84S mutations [denoted cNTnC(C35S/C84S)] was used in this study. The engineering of the expression vector and the expression of ^{15}N-labeled proteins in *Escherichia coli* were as described previously (*19*). Two synthetic cTnI peptides, $cTnI_{147-163}$ (acetyl-RISADAMMQALLGARAK-amide) and $cTnI_{144-163}$ (acetyl-RRVRISADAMMQALLGARAK-amide), were obtained from GL Biochem Ltd. (Shanghai, China). The purity was verified by HPLC and the mass verified by electrospray mass spectrometry. CMDP, AMDP, MPDP, and imazodan were purchased from Sigma-Aldrich. AMDP and levosimendan were purchased from Kinbester Co. Ltd. (Hong Kong). CI-930 was obtained from Pfizer. Stock solutions of the compounds in DMSO-d_6 (Cambridge Isotopes Inc.) were prepared, and the vials containing the solutions were wrapped in aluminum foil due to sensitivity to light. All drug stock solutions were made fresh for every titration to minimize possible time-induced degradation. The concentrations were determined gravimetrically. All NMR samples were 500 μL in volume. The buffer conditions were 100 mM KCl, 10 mM imidazole, and 0.17 mM DSS in a 90% H_2O/10% D_2O mixture, and the pH was 6.7. DTT, NaN_3, and protease

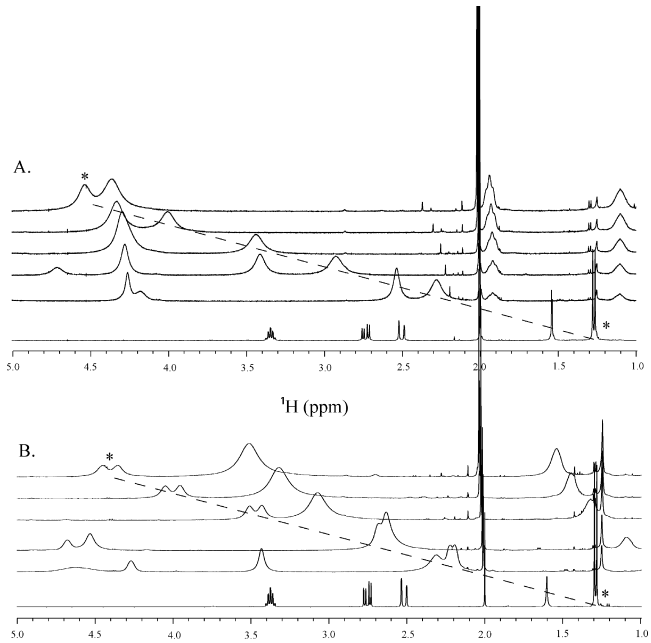

FIGURE 2: Stacked spectra of the titration of levosimendan (A) and CI-930 (B) with the shift reagent Eu-(hfc)$_3$ as monitored by 1D ^{1}H NMR spectroscopy. From bottom to top, the [Eu-(hfc)$_3$]/[CI-930] ratios for each titration point are 0, 0.25, 0.34, 0.54, 0.72, and 0.84, respectively. In the levosimendan titration series (A), no splitting of the methyl resonance (*) is observed, while in the case of CI-930 (B), splitting of the methyl resonance (*) is noticed, indicating an *R*/*S* mixture of enantiomers with roughly equal concentrations.

inhibitor cocktail were not used to prevent possible interactions with the drug compounds. Hamilton syringes and Gilson Pipetman P2 and P10 were used to deliver the drug solutions for all titrations.

Compound Stereospecificity. The chiral lanthanide shift reagent Eu-(hfc)$_3$ (Sigma-Aldrich) was titrated into NMR samples (all in $CDCl_3$, Cambridge Isotopes Inc.) of levosimendan, CMDP, AMDP, and CI-930 to determine whether the methyl on the pyridazinone ring was stereospecific or if the compounds were enantiomer mixtures (for a review, see ref *20*). All of the NMR spectra were obtained using a Varian INOVA 500 MHz spectrometer at 30 °C. A 500 μL sample volume was used for each compound, and TMS was used to reference the spectra at 0 ppm. For each titration, 16 transients were acquired at each point. A 16.5 mM sample of CI-930 was prepared, and a 0.27 M stock solution of Eu-(hfc)$_3$ was titrated into the solution at concentrations of 0.43, 0.86, 1.4, 1.94, 3.02, 4.1, 5.18, 6.26, 7.34, 8.42, 9.23, 12.47, and 15.17 mM. A 17 mM CMDP sample was prepared and titrated with a 0.322 M stock solution of Eu-(hfc)$_3$ to yield Eu-(hfc)$_3$ concentrations of 1.28, 1.93, 2.6, 3.22, 4.5, 5.8, 11.6, and 17.6 mM. A 13.6 mM AMDP sample was prepared and titrated with a 0.4 M stock solution of Eu-(hfc)$_3$ to yield final concentrations of 1.73, 3.44, 5.14, 6.82, 8.5, and 10.2 mM. A 10 mM levosimendan sample was prepared, and aliquots of Eu-(hfc)$_3$ were added to the sample to yield 1.82, 3.6, 5.4, 7.18, and 8.65 mM Eu-(hfc)$_3$. The one-dimensional (1D) ^{1}H NMR spectrum of each compound was assigned, and the methyl was monitored throughout the titration with chiral shift reagent Eu-(hfc)$_3$ (Figure 2). The NMR signal from the methyl of levosimendan did not undergo splitting during the titration with Eu-(hfc)$_3$, indicating that the drug was of pure *R* stereospecificity (Figure 2A). Meanwhile, the titration of Eu-(hfc)$_3$ into the NMR samples of CMDP, AMDP, and CI-930 revealed a splitting of the methyl resonance, indicating that these compounds are racemic mixtures of roughly equal *R* and *S* components (Figure 2B).

Titration of cNTnC(C35S/C84S)·Ca^{2+} with cTnI$_{147-163}$ and cNTnC(C35S/C84S)·Ca^{2+} with cTnI$_{144-163}$. The titration of [^{15}N]cNTnC(WT)·Ca^{2+} with cTnI$_{147-163}$ was conducted previously (*6*), and the titration of [^{15}N]cNTnC(C35S/C84S)·Ca^{2+} (0.6 and 0.7 mM, respectively) with cTnI$_{147-163}$ and cTnI$_{144-163}$ was done in this work. Both cTnI$_{147-163}$ and cTnI$_{144-163}$ are highly soluble in aqueous solution but tend to form gels at high concentrations, likely due to aggregation. Thus, no stock solution was prepared; instead, solid peptide was added at every titration point. The concentrations of [^{15}N]cNTnC(C35S/C84S)·Ca^{2+} and the peptides were determined by amino acid analysis at every titration point, giving the peptide/protein ratios. The decrease in pH associated with peptide additions was offset by adjusting the pH to 6.7 at every titration point. Both 1D ^{1}H and 2D ^{1}H$-^{15}$N HSQC NMR spectra were acquired and analyzed at every titration point. Like in the titration of [^{15}N]cNTnC(WT)·Ca^{2+} with cTnI$_{147-163}$ (*6*), 3$-$3.5 equiv of cTnI$_{147-163}$ is required to saturate [^{15}N]cNTnC(C35S/C84S)·Ca^{2+}, whereas 1$-$1.1 equiv of cTnI$_{144-163}$ is required to saturate [^{15}N]cNTnC(C35S/C84S)·Ca^{2+}.

Titration of cNTnC(C35S/C84S)·Ca^{2+}·cTnI$_{147-163}$ and cNTnC(C35S/C84S)·Ca^{2+}·cTnI$_{144-163}$ with Levosimendan, CMDP, AMDP, CI-930, Imazodan, and MPDP. The [^{15}N]cNTnC(C35S/C84S)·Ca^{2+}·cTnI$_{147-163}$ complex was formed by dissolving 1 equiv of solid protein (0.8 mM) and ~3.5 equiv of solid peptide (2.8 mM) in NMR buffer, and the [^{15}N]cNTnC(C35S/C84S)·Ca^{2+}·cTnI$_{144-163}$ complex was formed by dissolving 1 equiv of solid protein (1.0 mM) and ~1.1 equiv of solid peptide (1.1 mM) in NMR buffer. For both complexes, 4 equiv of $CaCl_2$ was added to saturate cNTnC, the pH was adjusted to 6.7, and a slight amount of precipitate was eliminated by filtration. The final NMR sample volume was 500 μL. The protein and peptide concentrations were determined gravimetrically and calibrated on the basis of amino acid analysis of each individual component. Both 1D ^{1}H and 2D ^{1}H$-^{15}$N HSQC NMR spectra were acquired and analyzed at every titration point.

A stock solution of 97 mM levosimendan was used for the titration of [^{15}N]cNTnC(C35S/C84S)·Ca^{2+}·cTnI$_{147-163}$ in aliquots of 1.0, 1.0, 1.0, 1.0, 2.0, 4.0, 4.0, and 4.0 μL. A stock solution of 95 mM levosimendan was used for the titration of [^{15}N]cNTnC(C35S/C84S)·Ca^{2+}·cTnI$_{144-163}$ in volumes of 1.0, 2.0, 5.0, 5.0, 10.0, and 10.0 μL. The sample was mixed thoroughly with each addition. In both cases, levosimendan started to precipitate when the drug to protein ratio reached ~4/1. This precipitate is likely unbound levosimendan, which is insoluble in aqueous solution. The titrations were stopped shortly after the appearance of precipitation. Addition of levosimendan slightly decreased the pH, which was adjusted by adding 1 M NaOH to NMR samples.

Aliquots of 1 μL of a 100 mM CMDP stock solution were added to [^{15}N]cNTnC(C35S/C84S)·Ca^{2+}·cTnI$_{147-163}$ and [^{15}N]cNTnC(C35S/C84S)·Ca^{2+}·cTnI$_{144-163}$. The titration was stopped when white precipitate started to appear (after the 8 μL addition). The change in pH from CMDP addition was negligible.

A stock of 100 mM AMDP was added in aliquots of 0.5, 1.5, 5.0, 5.0, 8.0, and 8.0 μL of [^{15}N]cNTnC(C35S/C84S)·Ca^{2+}·$cTnI_{147-163}$. AMDP is highly soluble in aqueous solution, and no precipitate was observed even after the final aliquot. A stock of 100 mM AMDP was added in aliquots of 0.5, 1.5, 5.0, 5.0, 8.0, and 10.0 μL to [^{15}N]cNTnC(C35S/C84S)·Ca^{2+}·$cTnI_{144-163}$. Again, no precipitate was observed during or after the titration. The change in pH from AMDP addition was negligible.

Into a NMR tube containing [^{15}N]cNTnC(C35S/C84S)·Ca^{2+}·$cTnI_{147-163}$ were titrated aliquots of 1.0, 5.0, 5.0, 5.0, 5.0, and 5.0 μL of a 100 mM CI-930 stock solution. To the [^{15}N]cNTnC(C35S/C84S)·Ca^{2+}·$cTnI_{144-163}$ complex were added aliquots of 0.25, 0.5, 2.5, 5.0, 5.0, 5.0, 5.0, and 5.0 μL of a 97 mM CI-930 stock solution. The change in pH from CI-930 addition was negligible.

Imazodan precipitated after an addition of 1 μL of a 100 mM stock solution to the NMR sample of either [^{15}N]-cNTnC(C35S/C84S)·Ca^{2+}·$cTnI_{147-163}$ or [^{15}N]cNTnC(C35S/C84S)·Ca^{2+}·$cTnI_{144-163}$. This was also the case with MPDP. Further additions resulted in more precipitation. No chemical shift changes were observed for the imazodan and MPDP titrations.

Pure DMSO-d_6 was added to a NMR sample containing [^{15}N]cNTnC(C35S/C84S) to test if it would induce chemical shift changes in [^{15}N]cNTnC(C35S/C84S). No chemical shift perturbations were observed in the 2D ^{1}H$-^{15}$N HSQC spectrum upon addition of DMSO-d_6 (data not shown). To confirm that levosimendan was not interacting with free $cTnI_{147-163}$ or $cTnI_{144-163}$, levosimendan was titrated into solutions containing either peptide. 1D ^{1}H NMR revealed no chemical shift change for $cTnI_{147-163}$ or $cTnI_{144-163}$ in the presence of levosimendan, when compared to the spectra acquired in the absence of the drug (data not shown).

NMR Spectroscopy. All of the NMR spectra were recorded using a Varian INOVA 500 MHz spectrometer at 30 °C. All 1D ^{1}H and 2D ^{1}H$-^{15}$N HSQC spectra were acquired using the water and gNhsqc.c pulse sequences, respectively (BioPack, Varian Inc.). The CBCA(CO)NNH and HNCACB NMR triple-resonance experiments (*21*) were conducted to determine backbone assignments of the [^{13}C,^{15}N]cNTnC·Ca^{2+}·$cTnI_{144-163}$ complex. Spectral processing was accomplished with VNMRJ (version 2.1B, Varian Inc.) and NMRPipe (*22*) and referenced according to the IUPAC conventions. Processed NMR spectra were analyzed using NMRView (*23*), and the backbone assignment of [^{13}C,^{15}N]cNTnC·Ca^{2+}·$cTnI_{144-163}$ complex was accomplished with the aid of Smartnotebook (*24*).

RESULTS

Throughout this study, 2D ^{1}H$-^{15}$N HSQC NMR spectra were used to monitor the binding of unlabeled ligands (such as the cTnI peptides, levosimendan, or its analogues) to ^{15}N-labeled cNTnC·Ca^{2+}. In these titrations, the chemical shifts of several assigned amide NH cross-peaks in the 2D ^{1}H$-^{15}$N HSQC NMR spectrum of [^{15}N]cNTnC·Ca^{2+} were perturbed as a function of added ligand. In addition to the identification of ligands that associate with the ^{15}N-labeled protein, the changes in residue specific backbone shifts, which can be quantified to derive ligand stoichiometry and affinity, can also be used to locate the ligand binding site on the protein. This procedure is commonly known as chemical shift mapping.

Interaction of cNTnC(C35S/C84S)·Ca^{2+} with $cTnI_{147-163}$ and $cTnI_{144-163}$. Previously, we titrated $cTnI_{147-163}$ into [^{15}N]cNTnC(WT)·Ca^{2+} and demonstrated that the binding of $cTnI_{147-163}$ to cNTnC(WT)·Ca^{2+} caused large chemical shift changes in the 2D ^{1}H$-^{15}$N HSQC NMR spectrum of the protein, consistent with the structural transition in cNTnC from a closed to an open state (*6*). The dissociation constant (K_D) of $cTnI_{147-163}$ for cNTnC(WT)·Ca^{2+} was determined to be 154 ± 10 μM. In this study, we found that the binding of $cTnI_{147-163}$ to cNTnC(C35S/C84S)·Ca^{2+} induced similar backbone amide ^{1}H or ^{15}N chemical shift changes, indicating a similar closed to open transition. The stoichiometry of binding of $cTnI_{147-163}$ to cNTnC·Ca^{2+} was 1/1 in both the WT and C35S/C84S isoforms. An expanded region of the 2D ^{1}H$-^{15}$N HSQC NMR spectra of cNTnC(C35S/C84S) free and in the cNTnC(C35S/C84S)·Ca^{2+}·$cTnI_{147-163}$ complex is depicted in Figure 3A, and peaks are labeled with residue assignments. Many peaks within this region of the spectrum, including V28, G34, V64, G68, and T71, moved in the $cTnI_{147-163}$ complex to characteristic chemical shifts corresponding to an open conformation of cNTnC(C35S/C84S) (shown by arrows connecting multiple and first single contours). When the longer peptide $cTnI_{144-163}$ was titrated into cNTnC(C35S/C84S)·Ca^{2+}, the majority of the cross-peaks in the 2D ^{1}H$-^{15}$N HSQC NMR spectrum of cNTnC(C35S/C84S) shifted along nearly identical pathways as in the titration of $cTnI_{147-163}$ into cNTnC(C35S/C84S)·Ca^{2+} but farther (shown by arrows connecting multiple and second single contours). The 2D ^{1}H$-^{15}$N HSQC NMR spectrum of cNTnC(C35S/C84S) in the cNTnC(C35S/C84S)·Ca^{2+}·$cTnI_{144-163}$ complex has been assigned, and the cross-peaks are labeled with residue assignments (Figure 3A). The pattern of spectral changes is very similar for the two complexes (Figure 3B) except for larger backbone amide ^{1}H or ^{15}N chemical shift perturbations of cNTnC(C35S/C84S) induced by $cTnI_{144-163}$ in comparison with $cTnI_{147-163}$. The additional movements of the residues indicate that the binding of $cTnI_{144-163}$ generates a more stable open conformation for cNTnC(C35S/C84S)·Ca^{2+} than $cTnI_{147-163}$. The average chemical shift changes of several residues that were perturbed the most during titration are plotted as a function of $[cTnI_{144-163}]_{total}$/$[cNTnC(C35S/C84S)\cdot Ca^{2+}]_{total}$ ratio (Figure 4), and the data were fit to the following equation:

$$cNTnC(C35S/C84S)\cdot Ca^{2+} + cTnI_{144-163} \rightleftarrows cNTnC(C35S/C84S)\cdot Ca^{2+}\cdot cTnI_{144-163}$$

This yielded a macroscopic dissociation constant of 15 ± 5 μM, which is 10 times smaller than the dissociation constant for $cTnI_{147-163}$ binding to cNTnC(WT)·Ca^{2+} (*6*).

Interaction of cNTnC(C35S/C84S)·Ca^{2+}·$cTnI_{147-163}$ and cNTnC(C35S/C84S)·Ca^{2+}·$cTnI_{144-163}$ with Levosimendan, CMDP, AMDP, and CI-930. The formation of the cNTnC-(C35S/C84S)·Ca^{2+}·$cTnI_{147-163}$ and cNTnC(C35S/C84S)·Ca^{2+}·$cTnI_{144-163}$ complexes were monitored by 2D ^{1}H$-^{15}$N HSQC NMR spectroscopy (Figure 3A). The assigned backbone amides of cNTnC(C35S/C84S) in the cNTnC(C35S/C84S)·Ca^{2+}·$cTnI_{147-163}$ and cNTnC(C35S/C84S)·Ca^{2+}·$cTnI_{144-163}$ complexes were then used to follow the titration

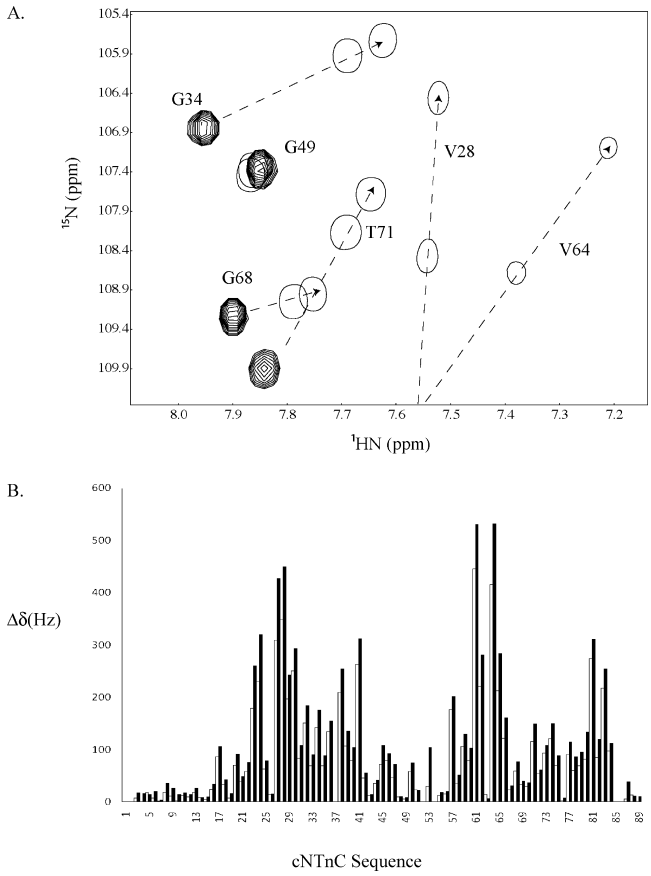

FIGURE 3: (A) Overlay of a well-dispersed region of the 2D $^{1}H-^{15}N$ HSQC NMR spectra of cNTnC(C35S/C84S)·Ca^{2+} (multiple contours), cNTnC(C35S/C84S)·Ca^{2+}·$cTnI_{147-163}$ (first single contour), and cNTnC(C35S/C84S)·Ca^{2+}·$cTnI_{144-163}$ (second single contour) complexes. The arrows indicate the direction of chemical shift change during titration of cTnI into cNTnC(C35S/C84S)·Ca^{2+}. Single contours represent the two cNTnC−cTnI complexes at the end points of titrations. The end points were determined by the cessation of chemical shift changes, which indicated a saturated complex. (B) $cTnI_{147-163}$-induced (white bars) and $cTnI_{144-163}$-induced (black bars) chemical shift changes of the backbone amides of cNTnC(C35S/C84S). Chemical shifts are presented in hertz and calculated as follows: $\Delta\delta = [(\Delta\delta_{^1H})^2 + (\Delta\delta_{^{15}N})^2]^{1/2}$. Since hertz is used instead of parts per million to calculate the total chemical shift changes ($\Delta\delta$), a correction factor of $^1/_5$ in the ^{15}N dimension is not needed.

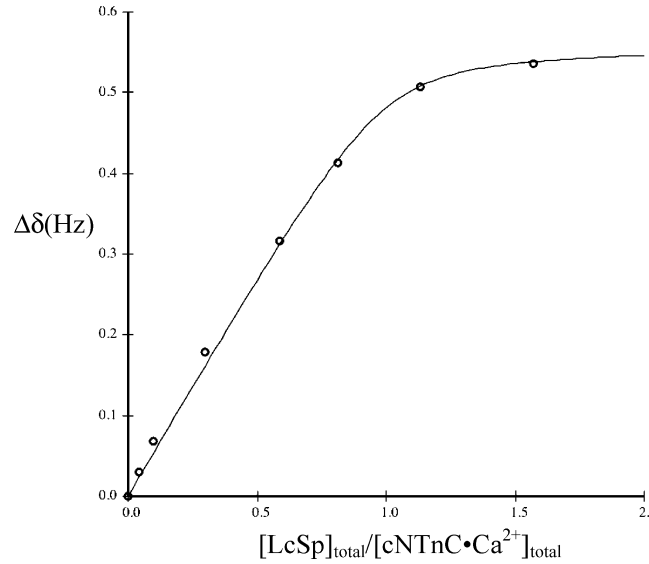

FIGURE 4: Titration of cNTnC(C35S/C84S)·Ca^{2+} with $cTnI_{144-163}$. The data are averaged over several residues with significant chemical shift changes observed during titration. The best-fit curve to the data is shown as a solid line. Conditions are described in Experimental Procedures.

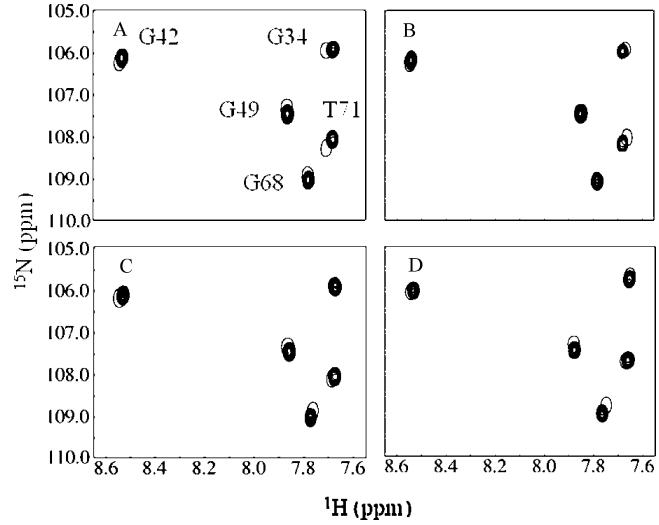

FIGURE 5: Titration of cNTnC(C35S/C84S)·Ca^{2+}·$cTnI_{144-163}$ [1.0 mM cNTnC(C35S/C84S) and 1.1 mM $cTnI_{144-163}$] with (A) levosimendan, (B) CMDP, (C) AMDP, and (D) CI-930 as monitored by 2D $^{1}H-^{15}N$ HSQC NMR spectroscopy. The region of the 2D $^{1}H-^{15}N$ HSQC spectrum with well-dispersed resonances is shown. Conditions are described in Experimental Procedures.

of levosimendan, CMDP, AMDP, and CI-930 (Figure 1). The initial (●) and end points (○) from the titrations of cNTnC(C35S/C84S)·Ca^{2+}·$cTnI_{144-163}$ with (A) levosimendan, (B) CMDP, (C) AMDP, and (D) CI-930 are shown in Figure 5. In contrast to the dramatic chemical shift changes induced by $cTnI_{147-163}$ or $cTnI_{144-163}$, those associated with drug binding are much smaller. This suggests that unlike the cTnI switch peptides, the drug compounds do not induce a large structural opening of cNTnC(C35S/C84S) but rather cause subtle perturbations on the interface between cNTnC(C35S/C84S) and the cTnI peptides. All four compounds induced backbone amide chemical shift changes in a common set of residues of both the cNTnC(C35S/C84S)·Ca^{2+}·$cTnI_{147-163}$ and cNTnC(C35S/C84S)·Ca^{2+}·$cTnI_{144-163}$ complexes. This suggests that the general location of binding is similar for these pyridazinone derivatives. It is interesting that although usually the same residues underwent perturbations throughout the different classes of ligands, the chemical shift changes were not always in the same direction. This may be due to the different moieties present on the various pyridazinone derivatives. To correlate the drug-induced chemical shift changes of cNTnC(C35S/C84S) to conformational changes in the protein, we plotted the changes for backbone atoms against the protein sequence (Figure 6). The magnitude of the changes was generally small but similar to those reported in levosimendan binding to cTnC·$3Ca^{2+}$ (*25*) and to cTnC·$3Ca^{2+}$·$cTnI_{32-79}$·$cTnI_{128-180}$ (*18*). The changes induced by levosimendan (Figure 6A) or CMDP (Figure 6B) were relatively larger (≤60 Hz) than those (≤20 Hz) induced by AMDP (Figure 6C) and CI-930 (Figure 6D). This indicates that the group attached to the aromatic ring [mesoxalonitrile hydrazone in levosimendan, chloro in CMDP, amino in AMDP, and imidazole in CI-930 (see Figure 1)] influences the drug−protein−peptide interaction.

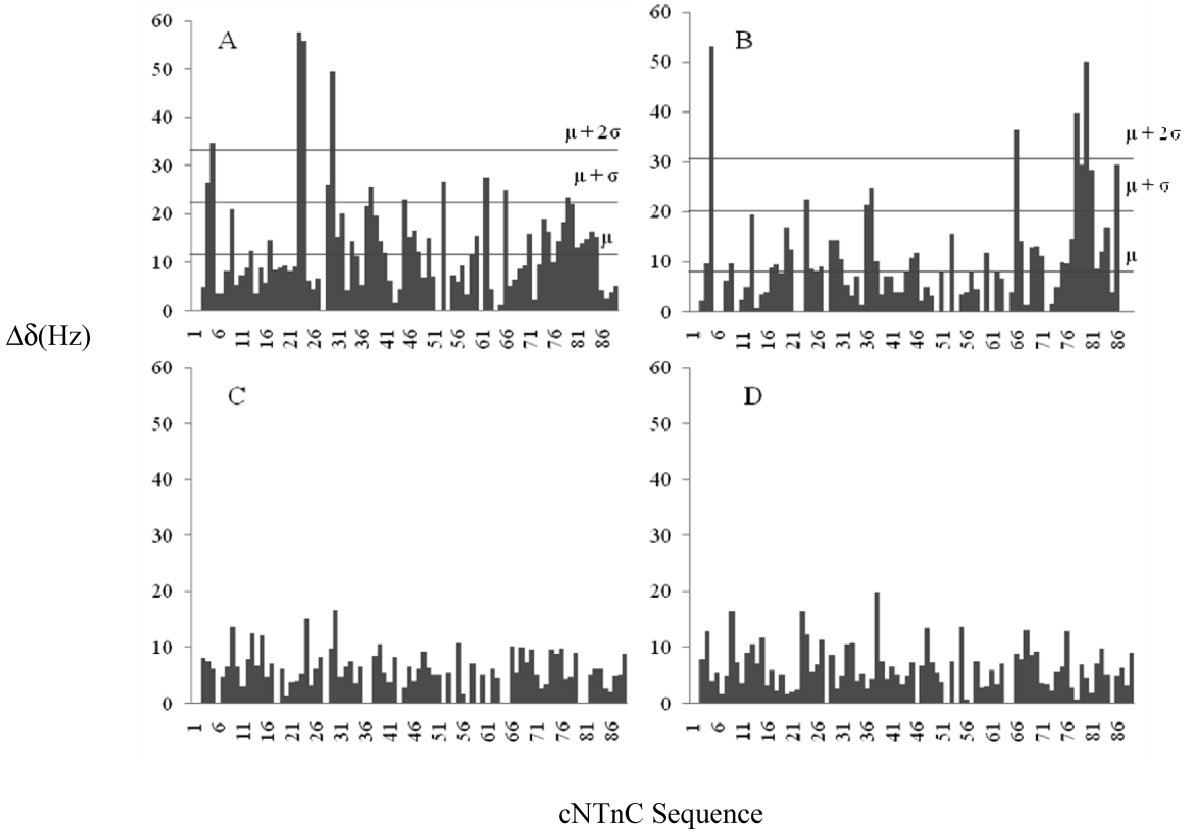

FIGURE 6: (A) Levosimendan, (B) CMDP, (C) AMDP, and (D) CI-930-induced chemical shift changes of the backbone amides of cNTnC(C35S/C84S) in the cNTnC(C35S/C84S)·Ca^{2+}·$cTnI_{144-163}$ complex [1.0 mM cNTnC(C35S/C84S) and 1.1 mM $cTnI_{144-163}$]. Chemical shift changes are presented in hertz and calculated as follows: $\Delta\delta = [(\Delta\delta_{^1H})^2 + (\Delta\delta_{^{15}N})^2]^{1/2}$. Since hertz is used instead of parts per million to calculate the total chemical shift changes ($\Delta\delta$), a correction factor of $^1/_5$ in the ^{15}N dimension is not needed. Horizontal lines in the levosimendan and CMDP bar diagrams (A and B) show total chemical shift perturbations larger than the mean (μ), the mean plus one standard deviation ($\mu + \sigma$), and the mean plus two standard deviations ($\mu + 2\sigma$). These values were used for chemical shift mapping.

These four molecules contain a chiral methyl group on the pyridazinone ring which may be in direct contact with the protein and involved in anchoring the drug molecules to cNTnC(C35S/C84S)·Ca^{2+}·$cTnI_{144-163}$. This is supported by the observation that cNTnC(C35S/C84S)·Ca^{2+}·$cTnI_{147-163}$ and cNTnC(C35S/C84S)·Ca^{2+}·$cTnI_{144-163}$ do not interact with imazodan or MPDP, as represented by the lack of chemical shift perturbations.

To elucidate the binding site of levosimendan on cNTnC(C35S/C84S)·Ca^{2+}·$cTnI_{144-163}$, chemical shift mapping is shown in Figure 7. The solution structure of cNTnC·Ca^{2+}·$cTnI_{147-163}$ [Protein Data Bank (PDB) entry 1MXL] was used to map the final chemical shift changes induced by the titration of levosimendan into cNTnC(C35S/C84S)·Ca^{2+}·$cTnI_{144-163}$. The chemical shift perturbations are mapped on the structure by magnitude such that the chemical shift changes for residues colored pink were greater than the mean (μ), the chemical shift changes for residues colored dark salmon were one standard deviation above the mean chemical shift change ($\mu + \sigma$), and the chemical shifts for residues colored red were two standard deviations above the mean ($\mu + 2\sigma$) (see Figure 6A). Chemical shift mapping of CMDP on the structure of cNTnC·Ca^{2+}·$cTnI_{147-163}$ (PDB entry 1MXL) resulted in a surface nearly identical to that of levosimendan.

Binding Affinity Determination. The calculation of the affinities of the different drugs is illustrated in Figure 8. Data analysis of the titration of CI-930 into cNTnC(C35S/C84S)·Ca^{2+}·$cTnI_{147-163}$ and cNTnC(C35S/C84S)·Ca^{2+}·$cTnI_{144-163}$ is shown as an example. An expanded region of 2D $^1H-^{15}N$ HSQC NMR spectral changes induced by CI-930 is shown in panels A and C of Figure 8. Plots of chemical shift changes of L48 as a function of $[CI\text{-}930]_{total}$/$[cNTnC(C35S/C84S)\cdot Ca^{2+}\cdot cTnI_{147-163}]_{total}$ and $[CI\text{-}930]_{total}$/$[cNTnC(C35S/C84S)\cdot Ca^{2+}\cdot cTnI_{144-163}]_{total}$ are shown in panels B and D of Figure 8, respectively. In both cases, no plateau could be reached in the titration even at high protein/drug ratios, indicating weak binding. A global fitting approach (www.bionmr.ualberta.ca/bds/software/xcrvfit) was used, in which the data for residues perturbed during titration were fit to the following equation:

$$\text{protein} + \text{drug} \rightleftarrows \text{protein·drug}$$

yielding a K_D of 11 mM for CI-930 binding to cNTnC(C35S/C84S)·Ca^{2+}·$cTnI_{147-163}$ and 2.65 mM for CI-930 binding cNTnC(C35S/C84S)·Ca^{2+}·$cTnI_{144-163}$. For levosimendan, the K_D values are 8 and 0.7 mM, respectively, and for AMDP, those are 6.5 and 1.5 mM, respectively. We were not able to obtain the dissociation constants for CMDP due to the precipitation of the ligand prior to reaching a 1/1 stoichiometry. The results for levosimendan, AMDP, and CI-930 demonstrate that cNTnC(C35S/C84S)·Ca^{2+}·$cTnI_{144-163}$ presents a more complete binding site for the drug molecules than cNTnC(C35S/C84S)·Ca^{2+}·$cTnI_{147-163}$.

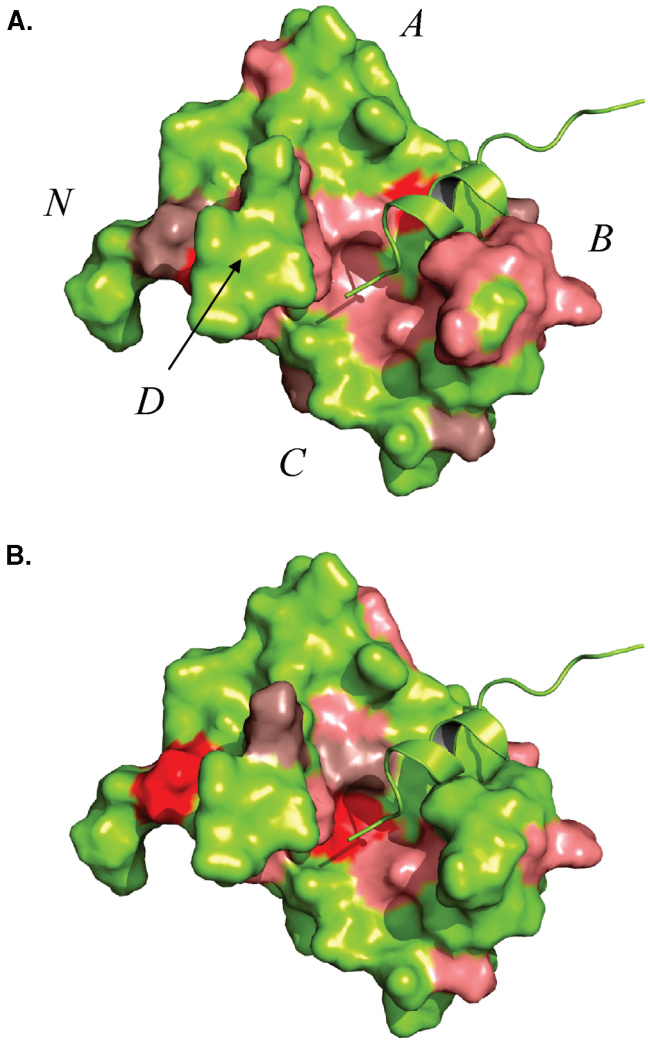

FIGURE 7: Surface representations of cNTnC·Ca^{2+}·$cTnI_{147-163}$ (PDB entry 1MXL). The cNTnC·Ca^{2+}·$cTnI_{147-163}$ complex is colored yellow with the helices of troponin C labeled. cNTnC·Ca^{2+} is depicted as a surface representation, whereas $cTnI_{147-163}$ is shown in ribbon format. Chemical shift perturbations induced by levosimendan (A) and CMDP (B) binding to cNTnC·Ca^{2+}·$cTnI_{144-163}$ are colored on the basis of the magnitude of the chemical shift. Chemical shifts greater than the mean plus two standard deviations ($\mu + 2\sigma$) are colored red, greater than the mean plus one standard deviation ($\mu + \sigma$) dark salmon, and greater than the mean (μ) salmon.

DISCUSSION

The goal of this study was to define the binding site of levosimendan and several structural analogues (Figure 1) in the regulatory domain of cTnC in complex with the switch region of cTnI, as well as to gain insight into the particular pharmacophores responsible for the binding of the ligands to the cNTnC−cTnI complex. An attractive aspect of this complex is that the interaction between cNTnC and the switch region of cTnI is Ca^{2+}-sensitive and the binding of Ca^{2+} and the cTnI switch are coupled to the opening of the cNTnC hydrophobic pocket, revealing an important target for cardiotonic drugs. We utilized 2D $^{1}H-^{15}N$ HSQC NMR spectroscopy to monitor the formation of two cTnC−cTnI complexes, cNTnC(C35S/C84S)·Ca^{2+}·$cTnI_{147-163}$ and cNTnC(C35S/C84S)·Ca^{2+}·$cTnI_{144-163}$, and the titration of six drug compounds to those complexes. Since 2D $^{1}H-^{15}N$ HSQC NMR spectroscopy can report information pertaining to individual atoms throughout the protein sequence, we were able to detect the subtle chemical shift changes of drug binding on the backbone amides of cNTnC(C35S/C84S) in the presence of $cTnI_{147-163}$ or $cTnI_{144-163}$ peptides. These measurements allowed the identification of a combination of specific amino acids in cNTnC and cTnI that form a binding pocket to accommodate the chiral methyl group on the pyridazinone ring of levosimendan and its analogues.

The structure of the cNTnC−cTnI complex has been characterized in several studies. We have shown that the binding of $cTnI_{147-163}$ induces a structural opening in cNTnC·Ca^{2+} (*6*). In the structure of cNTnC·Ca^{2+}·$cTnI_{147-163}$, the bound $cTnI_{147-163}$ peptide adopts an α-helical conformation spanning residues 4−12 in the 17-residue peptide. With the N-terminus of the peptide interacting with the center of the hydrophobic pocket, the α-helical region interacts with the AB helical interface and stabilizes the opening conformation of cNTnC·Ca^{2+}. The corresponding $sTnI_{115-131}$ peptide adopts a similar structure and a similar mode of interaction with sNTnC as observed in the structure of sNTnC(rhodamine)·$2Ca^{2+}$·$sTnI_{115-131}$ (*26*). The backbone atoms of the cNTnC·Ca^{2+}·$cTnI_{147-163}$ structure superimpose to 1.5 Å with the corresponding regions in the X-ray structure of the cardiac troponin complex cTnC·$3Ca^{2+}$·$cTnI_{31-210}$·$cTnT_{183-288}$. Addition of bepridil to cNTnC·Ca^{2+}·$cTnI_{147-163}$ resulted in the cNTnC·Ca^{2+}·$cTnI_{147-163}$·bepridil ternary complex, with the binding site for $cTnI_{147-163}$ primarily located on the AB interhelical interface and the binding site for bepridil in the center of the hydrophobic pocket (*16*). A similar binding scenario was observed in the X-ray structure of the sTnC·$4Ca^{2+}$·$sTnI_{1-182}$·$sTnT_{156-262}$ complex (*8*), in which a detergent molecule, anapoe, was found to bind together with the switch region of sTnI to sNTnC·$2Ca^{2+}$ (*8*). In the structure of sTnC·$4Ca^{2+}$·$sTnI_{1-182}$·$sTnT_{156-262}$, the three-residue extension (R112, R113, and V114) in the N-terminus of $sTnI_{115-131}$ is involved in electrostatic contacts with a number of acidic residues in both the C and D helices of sNTnC (Figure 9), which may enhance the stability of the open conformation of sNTnC·$2Ca^{2+}$. Although R144, R145, and V146 are not visualized in the cNTnC·Ca^{2+}·$cTnI_{147-163}$ and cTnC·$3Ca^{2+}$·$cTnI_{31-210}$·$cTnT_{183-288}$ structures, these residues were expected to be located in the proximity of the corresponding acidic residues, D87 and D88, in the D helix of cNTnC. This is based on the observation that the binding of the switch region of TnI to the N domain of TnC is the same in all the structures mentioned above. Thus, it is reasonable to suggest that cNTnC·Ca^{2+}·$cTnI_{144-163}$ would present a more stable complex with a higher-affinity binding site for drug compounds than cNTnC·Ca^{2+}·$cTnI_{147-163}$. This is in line with the observation in this work.

An earlier study has shown that the binding site of levosimendan is in the N domain of Ca^{2+}-saturated cTnC (*27*), although this was challenged by a different analysis showing that levosimendan did not bind to cTnC or a cTnC−cTnI complex (*28*). The later report showed that the inability to observe the levosimendan binding to cTnC was in part due to sample degradation and the use of a recombinant cTnC with C35 and C84 mutated to serines (*25*). It suggested that C84 is necessary for the interaction of levosimendan and cTnC. Furthermore, this report showed that levosimendan is capable of binding to both domains of

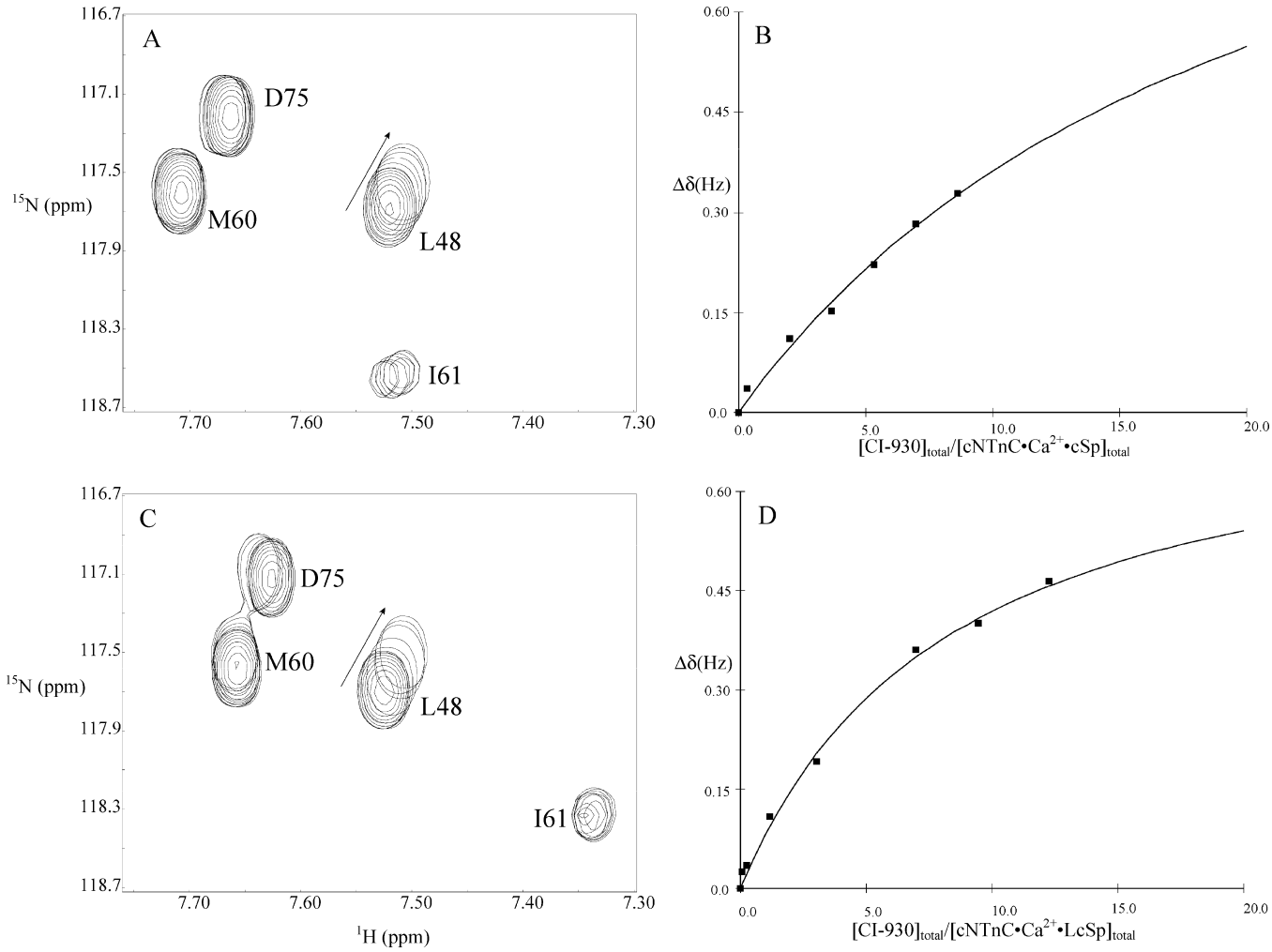

FIGURE 8: Selected region of 2D ^{1}H−^{15}N HSQC NMR spectra demonstrating the progressive shifts of L48 during the CI-930 titration to cNTnC(C35S/C84S)•Ca^{2+}•cTnI$_{147-163}$ (A) and to cNTnC(C35S/C84S)•Ca^{2+}•cTnI$_{144-163}$ (C). Chemical shift changes of L48 were plotted as a function of [CI-930]$_{total}$/[cNTnC(C35S/C84S)•Ca^{2+}•cTnI$_{147-163}$]$_{total}$ (B) and [CI-930]$_{total}$/[cNTnC(C35S/C84S)•Ca^{2+}•cTnI$_{144-163}$]$_{total}$ (D). The best-fit curves to the data are shown as solid lines.

cTnC. A recent investigation by Sorsa et al. (*18*) used NMR to demonstrate that levosimendan bound to only the N domain of cTnC in the presence of cTnI$_{32-79}$ and cTnI$_{128-180}$. Levosimendan-induced amide chemical shift changes were detected throughout the N domain of cTnC in the presence of the cTnI peptides. A number of N domain resonances either were broadened beyond detection or exhibited multiple chemical shifts. A large number of both polar and nonpolar residues that exhibited chemical shift changes upon levosimendan binding precluded identification of the levosimendan-binding site on cNTnC. Sorsa et al. (*18*) attributed the numerous N domain chemical shift changes to levosimendan altering either the dynamic equilibrium or the rate of exchange between open and closed N domain conformations by partially stabilizing defunct Ca^{2+} site I in cNTnC•Ca^{2+}. The exact binding location of levosimendan on cTnC remained unclear, although all the studies cited above suggested that its binding site is in the proximity of M81, M85, and F77 (residues on the D helix) within the hydrophobic pocket of cNTnC. Our data are in agreement with these studies and show that levosimendan targets the hydrophobic pocket of cNTnC. The chemical shift mapping depicted in Figure 7 indicates that all backbone amide resonances perturbed modestly (colored salmon) belong to the residues in the hydrophobic pocket, whereas the residues that are more significantly perturbed (colored dark salmon and red) belong to the N and A helices, away from the proposed binding surface. We suggest that the larger chemical shift perturbations of residues, such as Y5 and I4 on the N helix and A23 and F24 on the A helix, may be due to a slight conformational change of cNTnC•Ca^{2+}•cTnI$_{144-163}$ upon binding levosimendan, whereas the residues with smaller chemical shift changes identify the binding site of levosimendan in cNTnC•Ca^{2+}•cTnI$_{144-163}$ more accurately. The conformational change may be similar to that observed in the binding of bepridil to cNTnC•Ca^{2+}•cTnI$_{147-163}$, where in addition to the opening of cNTnC, there is a slight shift in the position of cTnI$_{147-163}$ (*15*). Our results demonstrated that the conserved positively charged N-terminal extension (RRV) in cTnI$_{144-163}$ is important for enhancing the affinity of levosimendan for cNTnC•Ca^{2+}. Thus, the network of electrostatic interactions between R144 and R145 of cTnI and D87 and D88 of cNTnC and the hydrophobic interactions between the helical region of cTnI$_{147-163}$ and the hydrophobic surface of cNTnC•Ca^{2+} create the levosimendan binding site with enhanced affinity, with a net result of the stabilization of the hydrophobic pocket and the open conformation of cNTnC•Ca^{2+}. We propose that the position

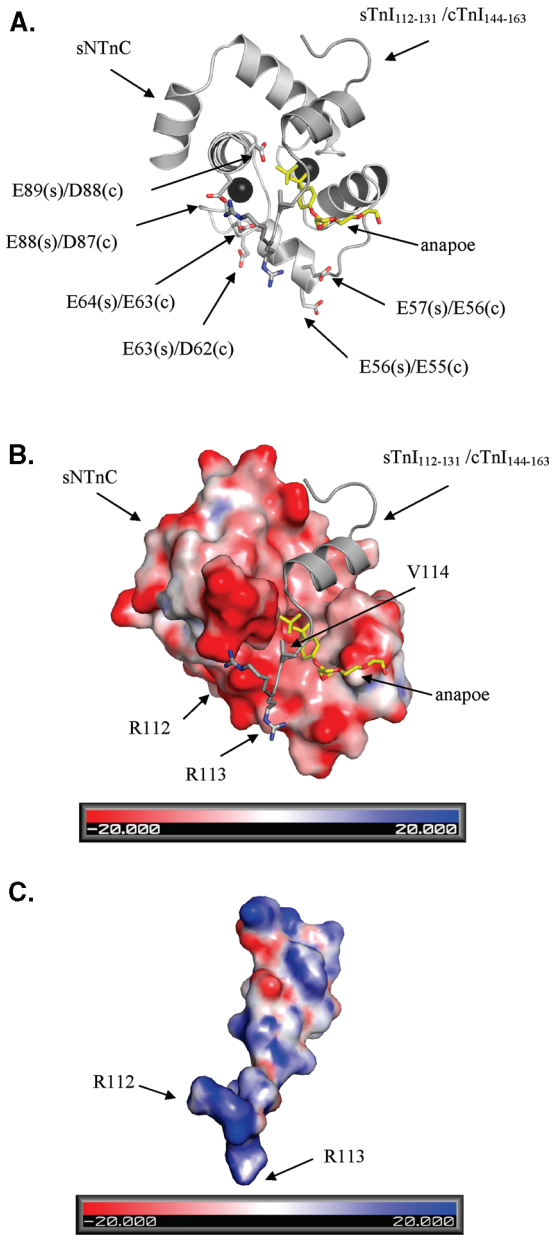

FIGURE 9: (A) Ribbon diagram of sNTnC·2Ca^{2+}·$sTnI_{112-131}$·anapoe (PDB entry 1YTZ). sNTnC is colored light gray, $sTnI_{112-132}$ dark gray, anapoe yellow, and calcium black. Six negatively charged residues of sNTnC (s) and cNTnC (c) are labeled. (B) Electrostatic surface map of sNTnC, with the potential contours shown at +20 k_BT/e (blue) and −20 k_BT/e (red). $sTnI_{112-131}$ is colored dark gray and shown as a ribbon diagram, with the three extra residues from the inhibitory region of sTnI, R112, R113, and V114, depicted as sticks. (C) Electrostatic surface map of $sTnI_{112-131}$, with the potential contours shown at +20 k_BT/e (blue) and −20 k_BT/e (red). Positively charged R112 and R113 are labeled on the electrostatic surface map. Surface maps were generated with ABPS (*41*).

of levosimendan in the cardiac troponin complex is analogous to that of anapoe in the skeletal troponin complex (Figure 9) on the basis of the results of chemical shift mapping (Figures 7). The A-Cys version of cNTnC was used in this study, and our results show that a cTnC−cTnI complex provides a favorable binding site for levosimendan in the absence of C84. The study (*25*) reporting that C84 is critical for the interaction of levosimendan and cNTnC suggested that the C84S mutation may slightly alter the conformation of the D helix of cNTnC to render the levosimendan binding site unavailable. Our results show that electrostatic interactions between R144 and R145 of cTnI and D87 and D88 of cNTnC help to stabilize the D helix and thereby the binding site for levosimendan. Covalent modification of C84 by levosimendan provides a plausible mechanism to account for the levosimendan-dependent effects (e.g., splitting of NMR peaks) observed by Sorsa et al. (*25*). This potential covalent interaction between C84 and levosimendan may not be required for its binding to the troponin complex but may subsequently occur in vivo (*29*).

To understand the effect of the pharmacophores of levosimendan on binding to cNTnC, we investigated the binding of several levosimendan analogues (Figure 1) to cNTnC·Ca^{2+}·$cTnI_{147-163}$ and cNTnC·Ca^{2+}·$cTnI_{144-163}$. Among the derivatives, only those containing the chiral methyl group induced chemical shift changes, suggesting that this group constitutes a key pharmacophore responsible for the binding of pyridazinone derivatives to cNTnC(C35S/C84S)·Ca^{2+}. This is probably because this methyl group contributes to the hydrophobic packing in a stereospecific manner. This type of interaction is demonstrated in the binding of EMD 57033 to the C domain of cTnC (*30, 31*). In the structure of cCTnC·2Ca^{2+}·EMD 57033, the drug molecule is oriented such that the chiral methyl group of EMD 57033 fits deep in the hydrophobic pocket and makes several key contacts with the protein. This stereospecifc interaction explains why the (−)-enantiomer of EMD 57033 (EMD 57439) is inactive. Studies on the action of stereoisomers of simendan (levosimendan and its + enantiomer, dextrosimendan) on cTnC have presented evidence that the Ca^{2+} sensitizing effect of levosimendan is in part due to a stereoselective binding to the N domain of cTnC (*32*). Another cardiotonic drug with structural characteristics similar to those of levosimendan, pimobendan, binds troponin and increases calcium sensitivity in a stereospecific manner as well (*33, 34*). The three levosimendan analogues that associated with cNTnC·Ca^{2+}·$cTnI_{147-163}$ and cNTnC·Ca^{2+}·$cTnI_{144-163}$, CMDP, AMDP, and CI-930 were shown in this work to be *R*/*S* mixtures (Figure 2); therefore, we cannot unambiguously conclude that binding to the complex is selective for one enantiomer over the other. However, it is possible that the affinity of one of the enantiomers of the pyridazinone compounds with cNTnC·Ca^{2+}·$cTnI_{144-163}$ is higher than that of the other.

In addition to the chiral methyl group on the pyridazinone ring, a group attached to the benzene ring may also be important in the binding. In levosimendan, this is a bulky group comprised of the mesoxalonitrile hydrazone moiety. Structure−activity analysis of levosimendan analogues has shown that this group is involved in hydrogen bonding with cTnC, indicating that both hydrogen bonds and van der Waals contacts are formed upon the binding of active levosimendan analogues to cTnC (*35*). Our data showed that levosimendan and CMDP induced larger chemical shift changes than AMDP and CI-930 (Figure 6). This demonstrates that the mesoxalonitrile hydrozone group in levosimendan and the chloro group in CMDP help to form stronger interactions with the binding site compared to the amino group in AMDP or the imidazole group in CI-930. Chemical shift mapping (Figure 7) identifies a similar binding site between levosimendan and CMDP located in the hydrophobic pocket of cNTnC·Ca^{2+}·$cTnI_{144-163}$. The large chemical

shift perturbations of residues residing on the N helix of cNTnC induced by CMDP suggest a structural opening of cNTnC·cTnI$_{144-163}$. The larger chemical shift changes of residues along the D helix of cNTnC from CMDP binding when compared with those of levosimendan may be due to the proximity of these residues to the electronegative chloro group of CMDP, or a slightly different binding mode between the ligands. The perturbed chemical shifts along the B helix induced by levosimendan may result from a larger displacement of cTnI$_{144-163}$ by the voluminous mesoxalonitrile hydrazone moiety when compared with CMDP. Assuming the binding mode of levosimendan and its analogues is similar to that of anapoe (Figure 9), the orientation of the pyridazinone molecules would be antiparallel to cTnI$_{144-163}$; i.e., the chiral methyl group on the pyridazinone ring fits deep in the hydrophobic cavity, whereas the group attached to the aromatic ring makes contacts with the residues in the N-terminus of cTnI$_{144-163}$ and the D helix of cNTnC. Interestingly, EMD 57033 also binds to the hydrophobic pocket of cCTnC in a similar manner, with the chiral methyl group deep inside the protein core.

The affinities determined for the binding of levosimendan ($K_D \sim 0.7$ mM), AMDP ($K_D \sim 1.5$ mM), and CI-930 ($K_D \sim 2.6$ mM) to cNTnC·Ca^{2+}·cTnI$_{144-163}$ are comparable to those from the previous studies on levosimendan binding to cTnC·3Ca^{2+}·cTnI$_{32-79}$·cTnI$_{128-180}$ ($K_D \geq 0.2$ mM) (*18*), W7 binding to cTnC·3Ca^{2+}·cTnI$_{34-71}$·cTnI$_{128-163}$ ($K_D \sim 0.5$ mM) (*17*), and anapoe binding to sTnC·4Ca^{2+}·sTnI$_{1-182}$·sTnT$_{156-262}$ ($K_D \sim 0.64$ mM) (*8*). This might support the notion that the binding of cardiotonic drugs to the regulatory unit of cardiac troponin occurs in a similar mode. These K_D values are in the high micromolar range, which is generally considered weak for protein−drug interactions. Levosimendan is known to exert multiple effects on perfused hearts at concentrations as low as 0.3 μM; the effect of levosimendan on skinned muscle fibers was half-maximal by 0.3 μM and maximal by 10 μM (*36*), and similar levels of levosimendan modulated contractility in cardiomyocytes (*37*). Several factors could contribute to this phenomenon. Micellization of drug molecules in aqueous solutions has been shown to cause low apparent affinities (*38, 39*). It is possible that cTnC in the highly organized and cooperative myofilaments may have a higher affinity for levosimendan than it does when cTnC is isolated in solution. On the other hand, the weak levosimendan−cTnC interaction may allow the drug to gently modulate cardiac contractility in a rhythmic fashion so that cardiac relaxation is not compromised. This is in accordance with a study reporting a K_D of >2 mM for the interaction of pineal hormone melatonin and calmodulin. The low affinity has been used to explain many in vitro effects and pharmacological dosages of melatonin (*40*). The small chemical shift changes observed in this study suggest that these drug molecules do not induce large conformational changes in cNTnC·Ca^{2+}·cTnI$_{144-163}$. This feature is potentially useful for the rapid mapping of the drug molecules to the already determined structure of cNTnC·Ca^{2+}·cTnI$_{147-163}$ via measurement of the intermolecular NOE restraints between cNTnC·Ca^{2+}·cTnI$_{147-163}$ and the drug molecules, a project currently in progress in our laboratory.

ACKNOWLEDGMENT

We thank David Corson and Melissa Rakovszky for protein purification, Olivier Julien, Robert Boyko, and Ryan Hoffman for help using software such as nmrView and nmrPipe, Jeff Devries for NMR spectrometer maintenance, Jeffrey Way and Sean Walker from Reify Corp. for early discussions, and Pfizer for the gift of CI-930.

REFERENCES

1. Li, M. X., Wang, X., and Sykes, B. D. (2004) Structural based insights into the role of troponin in cardiac muscle pathophysiology. *J. Muscle Res. Cell Motil. 25*, 559–579.
2. Kobayashi, T., and Solaro, R. J. (2005) Calcium, thin filaments, and the integrative biology of cardiac contractility. *Annu. Rev. Physiol. 67*, 39–67.
3. Sia, S. K., Li, M. X., Spyracopoulos, L., Gagné, S. M., Liu, W., Putkey, J. A., and Sykes, B. D. (1997) NMR structure of cardiac troponin C reveals an unexpected closed regulatory domain. *J. Biol. Chem. 272*, 18216–18221.
4. Spyracopoulos, L., Li, M. X., Sia, S. K., Gagné, S. M., Chandra, M., Solaro, R. J., and Sykes, B. D. (1997) Calcium-induced structural transition in the regulatory domain of human cardiac troponin C. *Biochemistry 36*, 12138–12146.
5. McKay, R. T., Saltibus, L. F., Li, M. X., and Sykes, B. D. (2000) Energetics of the induced structural change in a Ca^{2+} regulatory protein: Ca^{2+} and troponin I peptide binding to the E41A mutant of the N-domain of skeletal troponin C. *Biochemistry 39*, 12731–12738.
6. Li, M. X., Spyracopoulos, L., and Sykes, B. D. (1999) Binding of cardiac troponin-I 147−163 induces a structural opening in human cardiac troponin-C. *Biochemistry 38*, 8289–8298.
7. Takeda, S., Yamashida, A., Maeda, K., and Maeda, Y. (2003) Structure of the core domain of human cardiac troponin in the Ca^{2+}-saturated form. *Nature 424*, 35–41.
8. Vinogradova, M. V., Stone, D. B., Malanina, G. G., Karatzaferi, C., Cooke, R., Mendelson, R. A., and Fletterick, R. J. (2005) Ca^{2+}-regulated structural changes in troponin. *Proc. Natl. Acad. Sci. U.S.A. 102*, 5038–5043.
9. Lindhout, D. A., and Sykes, B. D. (2003) Structure and dynamics of the C-domain of human cardiac troponin C in complex with the inhibitory region of human cardiac troponin I. *J. Biol. Chem. 278*, 27024–27034.
10. Lindhout, D. A., Boyko, R. F., Corson, D. C., Li, M. X., and Sykes, B. D. (2005) The role of electrostatics in the interaction of the inhibitory region of troponin I with troponin C. *Biochemistry 44*, 14750–14759.
11. Arteaga, G. M., Kobayashi, T., and Solaro, R. J. (2002) Molecular actions of drugs that sensitize cardiac myofilaments to Ca^{2+}. *Ann. Med. 34*, 248–258.
12. Rosevear, P. R., and Finley, N. (2003) Molecular mechanism of levosimendan action: an update. *J. Mol. Cell. Cardiol. 35*, 1011–1015.
13. Sorsa, T., Pollesello, P., and Solaro, R. J. (2004) The contractile apparatus as a target for drugs against heart failure: Interaction of levosimendan, a calcium sensitizer, with cardiac troponin C. *Mol. Cell. Biochem. 266*, 87–107.
14. Kass, D. A., and Solaro, R. J. (2006) Mechanisms and use of calcium-sensitizing agents in the failing heart. *Circulation 113*, 305–315.
15. Li, M. X., Robertson, I. M., and Sykes, B. D. (2008) Interaction of cardiac troponin with cardiotonic drugs: A structural perspective. *Biochem. Biophys. Res. Commun. 369*, 88–99.
16. Wang, X., Li, M. X., and Sykes, B. D. (2002) Structure of the regulatory N-domain of human cardiac troponin C in complex with human cardiac troponin I$_{147-163}$ and bepridil. *J. Biol. Chem. 277*, 31124–31133.
17. Li, M. X., Hoffman, R. M. B., and Sykes, B. D. (2006) Interaction of cardiac troponin C with calmodulin antagonist W7 in the presence of three functional regions of cardiac troponin I. *Biochemistry 45*, 9833–9840.
18. Sorsa, T., Pollesello, P., Permi, P., Drakenberg, T., and Kilpelainen, I. (2003) Interaction of levosimendan with cardiac troponin C in the presence of cardiac troponin I peptides. *J. Mol. Cell. Cardiol. 35*, 1055–1061.

19. Li, M. X., Saude, E. J., Wang, X., Pearlstone, J. R., Smillie, L. B., and Sykes, B. D. (2002) Kinetic studies of calcium and cardiac troponin I peptide binding to human cardiac troponin C using NMR spectroscopy. *Eur. Biophys. J. 31*, 245–256.
20. Parker, D. (1991) NMR determination of enantiomeric purity. *Chem. Rev. 91*, 1441–1457.
21. Muhandiram, D. R., and Kay, L. E. (1994) Gradient-enhanced triple-resonance three-dimensional NMR experiments with improved sensitivity. *J. Magn. Reson., Ser. B 103*, 203–216.
22. Delaglio, F., Grzesiek, S., Vuister, G. W., Zhu, G., Pfeifer, J., and Bax, A. (1995) NMRPipe: A multidimensional spectral processing system based on UNIX pipes. *J. Biomol. NMR 6*, 277–293.
23. Johnson, B. A., and Blevins, R. A. (1994) NMRView: A computer program for teh visualization and analysis of NMR data. *J. Biomol. NMR 4*, 603–614.
24. Slupsky, C. M., Boyko, R. F., Booth, V. K., and Sykes, B. D. (2003) Smartnotebook: A semi-automated approach to protein sequential NMR resonance assignments. *J. Biomol. NMR 27*, 313–321.
25. Sorsa, T., Heikkinen, S., Abbott, M. B., Abusamhadneh, E., Laakso, T., Tilgmann, C., Serimaa, R., Annila, A., Rosevear, P. R., Drakenberg, T., Pollesello, P., and Kilpelainen, I. (2001) Binding of levosimendan, a calcium sensitizer, to cardiac troponin C. *J. Biol. Chem. 276*, 9337–9343.
26. Mercier, P., Ferguson, R. E., Corrie, J. E., Trenthem, D. R., and Sykes, B. D. (2003) Structure and dynamics of rhodamine labeled N-domain of skeletal troponin C in complex with with skeletal troponin I 115−131. *Biochemistry 42*, 4333–4348.
27. Pollesello, P., Ovaska, M., Kaivola, J., Tilgmann, C., Lundstrom, K., Kalkkinen, N., Ulmanen, I., Nissinen, E., and Taskinen, J. (1994) Binding of a new Ca^{2+} sensitizer, levosimendan, to recombinant human cardiac troponin C. A molecular modelling, fluorescence probe, and proton nuclear magnetic resonance study. *J. Biol. Chem. 269*, 28584–28590.
28. Kleerekoper, Q., and Putkey, J. A. (1999) Drug binding to cardiac troponin C. *J. Biol. Chem. 274*, 23932–23939.
29. Lehtonen, L., and Põder, P. (2007) The utility of levosimendan in the treatment of heart failure. *Ann. Med. 39*, 2–17.
30. Li, M. X., Spyracopoulos, L., Beier, N., Putkey, J. A., and Sykes, B. D. (2000) Interaction of cardiac troponin C with Ca^{2+} sensitizer EMD 57033 and cardiac troponin I inhibitory peptide. *Biochemistry 39*, 8782–8790.
31. Wang, X., Li, M. X., Spyracopoulos, L., Beier, N., Chandra, M., Solaro, R. J., and Sykes, B. D. (2001) Structure of the C-domain of human cardiac troponin C in complex with the Ca^{2+} sensitizing drug EMD 57033. *J. Biol. Chem. 276*, 25456–25466.
32. Sorsa, T., Pollesello, P., Rosevear, P. R., Drakenberg, T., and Kilpeläinen, I. (2003) Stereoselective binding of levosimendan to cardiac troponin C causes Ca^{2+}-sensitization. *Eur. J. Pharmacol. 486*, 1–8.
33. Solaro, R. J., Fujino, K., and Sperelakis, N. (1989) The positive inotropic effect of pimobendan involves stereospecific increases in the calcium sensitivity of cardiac myofilaments. *J. Cardiovasc. Pharmacol. 14*, S7–S12.
34. Fujino, K., Sperelakis, N., and Solaro, R. J. (1988) Differential effects of D- and L-pimobendan on cardiac myofilament calcium sensitivity. *J. Pharmacol. Exp. Ther. 247*, 519–523.
35. Levijoki, J., Pollesello, P., Kaivola, J., Tilgmann, C., Sorsa, T., Annila, A., Kilpelainen, I., and Haikala, H. (2000) Further evidence for the cardiac troponin C mediated calcium sensitization by levosimendan: Structure-response and binding analysis with analogs of levosimnedan. *J. Mol. Cell. Cardiol. 32*, 479–491.
36. Edes, I., Kiss, E., Kitada, Y., Powers, F. M., Papp, J. G., Kranias, E. G., and Solaro, R. J. (1995) Effects of levosimendan, a cardiotonic agent targeted to troponin C, on cardiac function and on phosphorylation and Ca^{2+} sensitivity of cardiac myofibrils and sarcoplasmic reticulum in guinea pig heart. *Circ. Res. 77*, 107–113.
37. Sato, S., Talukder, M. A., Sugawara, H., Sawada, H., and Endoh, M. (1998) Effects of levosimendan on myocardial contractility and Ca^{2+} transients in aequorin-loaded right-ventricular papillary muscles and indo-1-loaded single ventricular cardiomyocytes of the rabbit. *J. Mol. Cell. Cardiol. 30*, 1115–1128.
38. Attwood, D., and Natarajan, R. (1981) Effect of pH on the micellar properties of amphiphilic drugs in aqueous solution. *J. Pharm. Pharmacol. 33*, 136–140.
39. Ravin, L. J., and Warren, R. J. (1971) Micelle formation and its significance in interpretation of NMR spectra of phenothiazine. *J. Pharm. Sci. 60*, 329.
40. Turjanski, A. G., Estrin, D. A., Rosenstein, R. E., McCormick, J. E., Martin, S. R., Pastore, A., Biekofsky, R. R., and Martorana, V. (2004) NMR and molecular dynamics studies of the interaction of melatonin with calmodulin. *Protein Sci. 13*, 2925–2938.
41. Baker, N. A., Sept, D., Joseph, S., Holst, M. J., and McCammon, J. A. (2001) Electrostatics of nanosystems: Application to microtubules and the ribosome. *Proc. Natl. Acad. Sci. U.S.A. 98*, 10037–10041.

BI800438K